Supporting Information

Experimental Section

Materials. Lithium sheet was obtained from China Energy Lithium Co., Ltd. Lithium bis(trifluoromethane) sulfonamide ($C_2F_6S_2O_4NLi$, 99%), succinonitrile ($C_4H_4N_2$, 99%), polyethylene oxide (average M_v of ~600,000), and N-methyl-2-pyrrolidinone (C_5H_9NO, 99%) were purchased from Aladdin Reagent. Poly(vinylidene fluoride-co-hexafluoropropylene) (average M_n of ~130,000) was purchased from Sigma-Aldrich. Methylene chloride (CH_2Cl_2, 99.5%) and acetone (C_3H_6O, 99.5%) were purchased from Sinopharm Chemical Reagent Co., Ltd. Ecoflex was provided by Shanghai smarttech Co., Ltd.

Synthesis of spinnable carbon nanotube array. The spinnable carbon nanotube (CNT) array with a thickness of ~220 μm was synthesized by chemical vapor deposition. A silicon wafer deposited with Fe (1.2 nm)/Al_2O_3 (3 nm) was used as the catalyst. Ethylene with a flowing rate of 90 sccm was used as the carbon source, and a gas mixture of argon (400 sccm) and hydrogen (30 sccm) was used as the carrier gas. The growth occurred at 740 ^oC for 10 min.

Characterization. The structures were characterized by scanning electron microscope (SEM, Hitachi FE-SEM S-4800 operated at 1 kV), optical microscopy (Olympus BX51), and X-ray diffraction (XRD, Bruker AXS D8). X-ray photoelectron spectroscopy was recorded on an AXIS ULTRA DLD XPS System with MONO Al source (Shimadzu Corp.). Photoelectron spectrometer was recorded by using monochromatic Al KR radiation under vacuum at 5×10^{-9} Pa. All of the binding energies were referred to the C1s peak at 284.6 eV of the surface adventitious carbon. The photographs were taken by a camera (Nikon, J1).

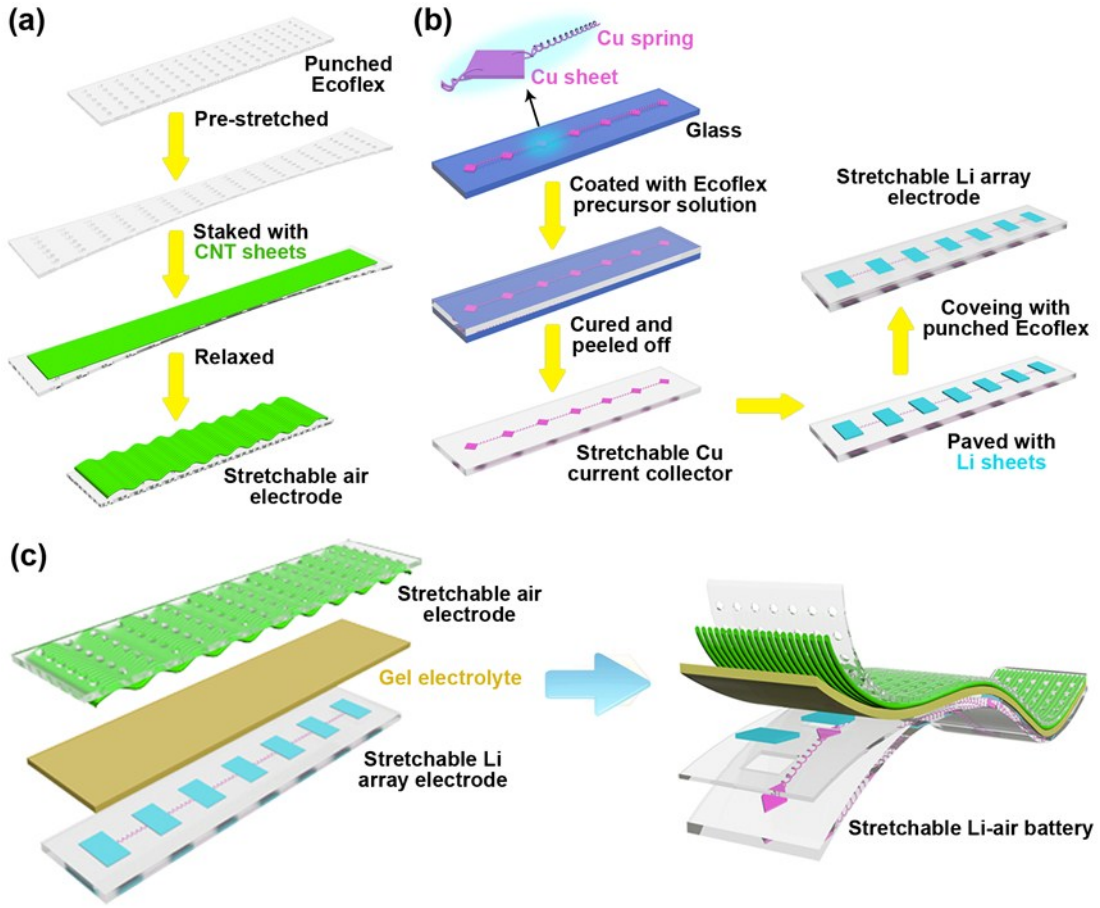

Figure S1. Schematic illustration to the fabrication of (**a**) stretchable air electrode, (**b**) stretchable Li array electrode, and (**c**) stretchable Li-air battery.

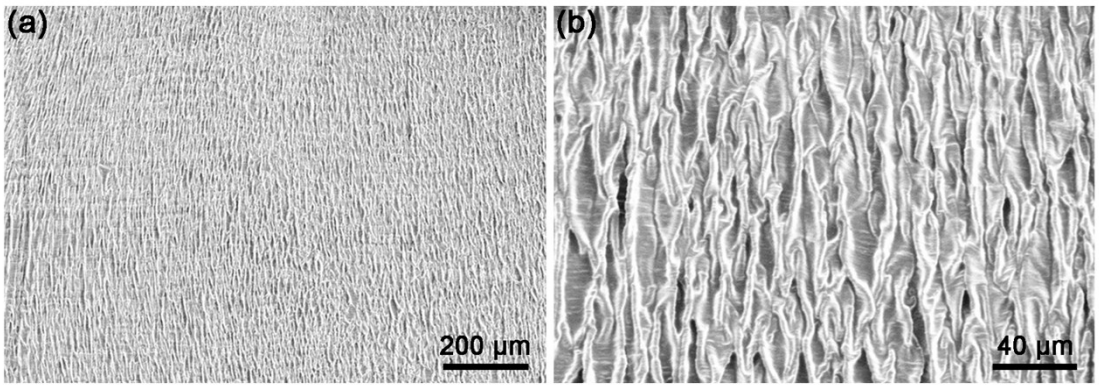

Figure S2. SEM images of the rippled CNT sheet at **(a)** low and **(b)** high magnifications.

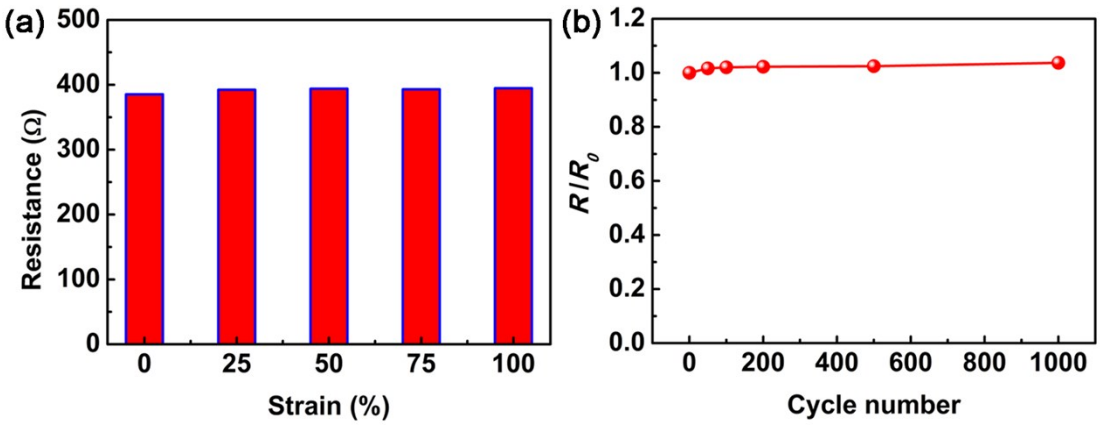

Figure S3. **a**) Dependence of electrical resistance of air electrode on strain. **b**) Dependence of electrical resistance of air electrode on stretching cycle number at a strain of 100%. Here R_0 and R correspond to the electrical resistances before and after stretching, respectively.

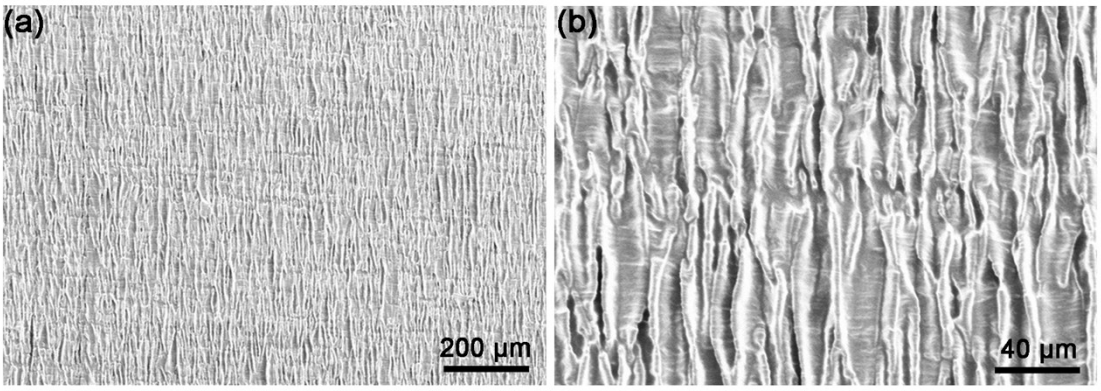

Figure S4. SEM images of the CNT sheets after 1000 cycles of stretching at a strain of 100% at **(a)** low and **(b)** high magnifications.

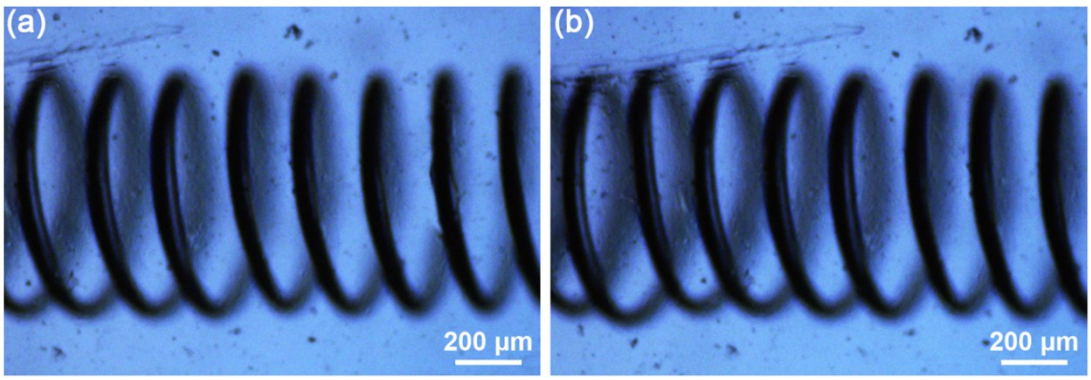

Figure S5. Optical micrographs of the embedded Cu spring **(a)** before and **(b)** after 1000 cycles of stretching at a strain of 100%.

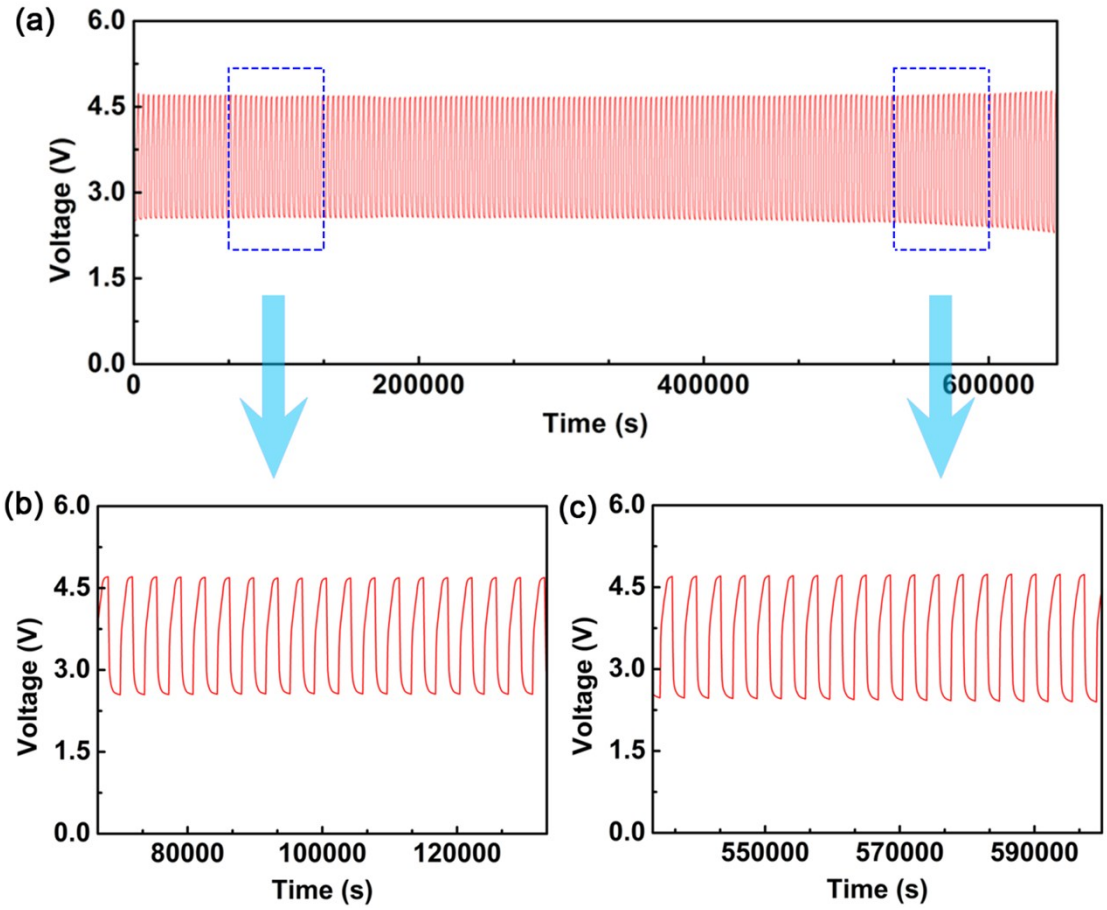

Figure S6. **a**) Galvanostatic cycling of a stretchable Li-air battery in the first 650,000 s. The current density was fixed at 1000 mA/g. **b**, **c**) Enlarged views from the blue dashed boxes.

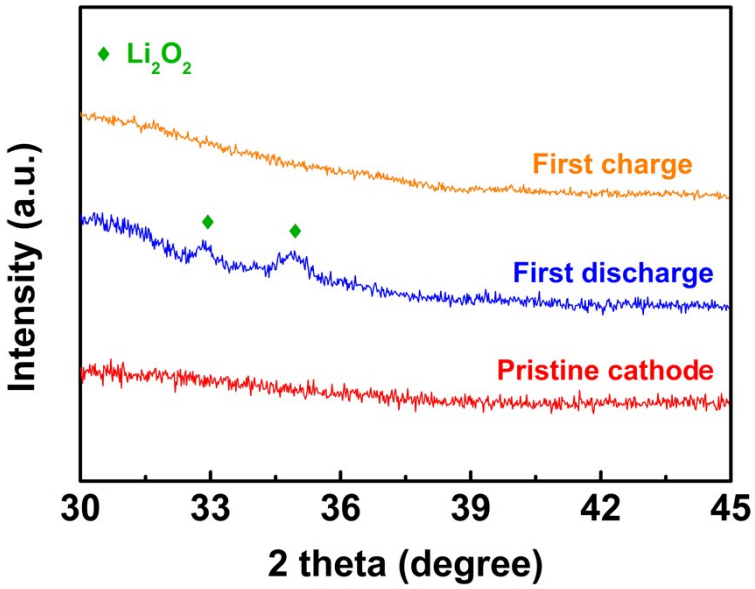

Figure S7. X-ray diffraction patterns of the cathode (air electrode) at different states.

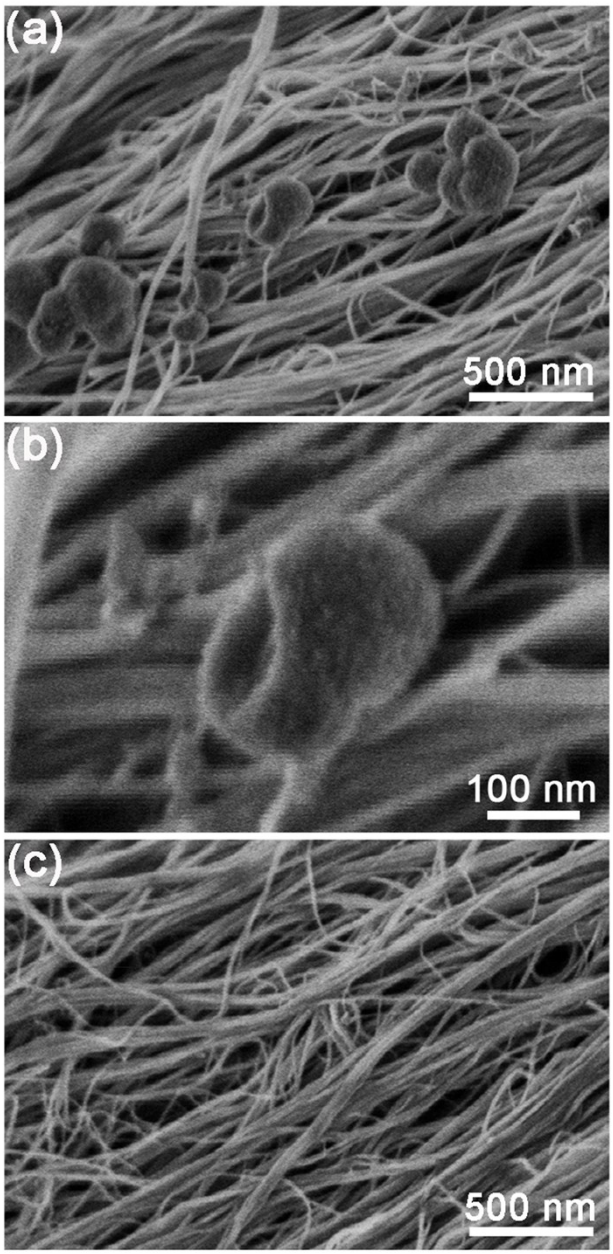

Figure S8. SEM images of the air electrode after the first (**a**, **b**) discharging and (**c**) recharging.

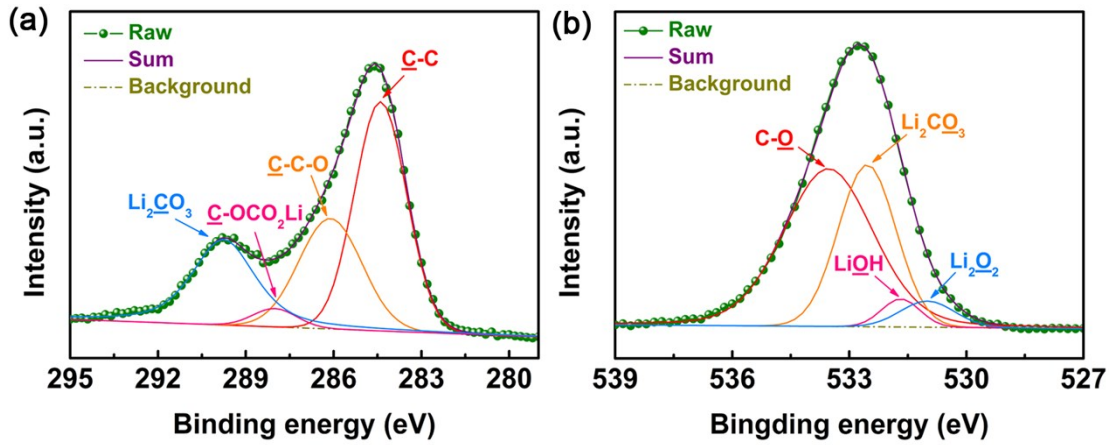

Figure S9. X-ray photoelectron spectroscopy characterizations of (**a**) C1s and (**b**) O1s signals of the CNT cathode after the 10th discharge in air.

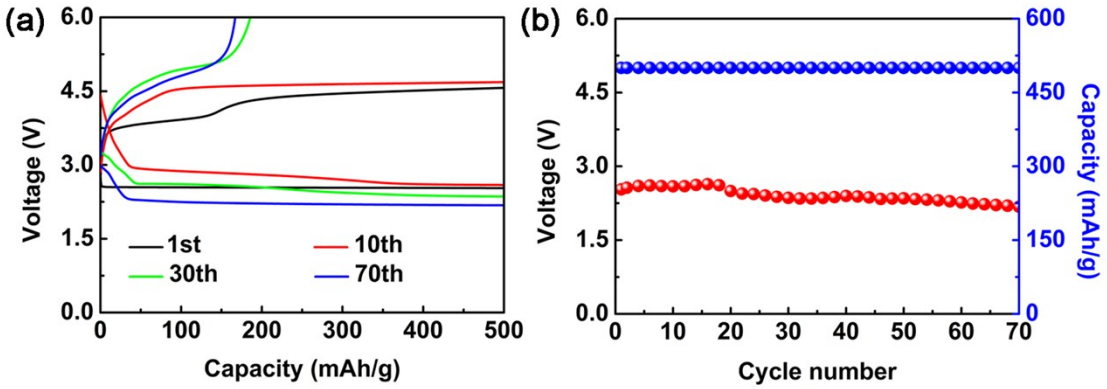

Figure S10. (**a**) Charge and discharge curves and (**b**) the corresponding cycling performance of the Li-air battery in ambient air with a relative humidity of ~20% at room temperature. The charge and discharge curves were measured at a current density of 1000 mA/g.

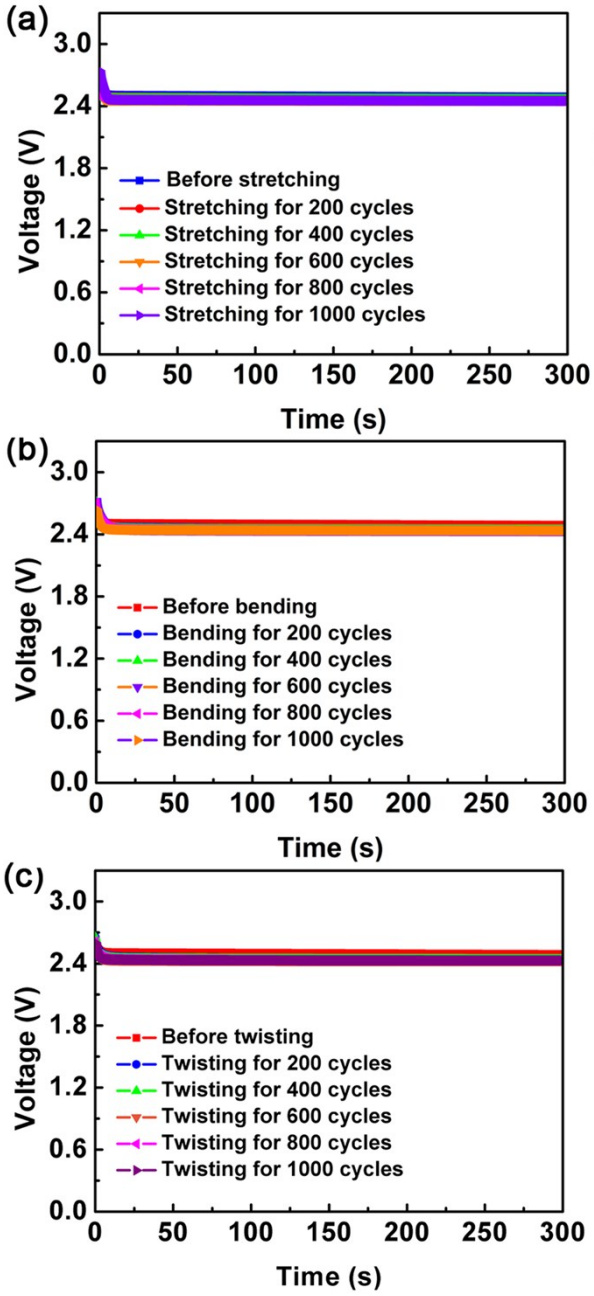

Figure S11. Dependence of the discharge voltage of a stretchable Li-air battery on (**a**) stretching cycle at a strain of 75%, (**b**) bending cycle at a bending angle of 90^{o} and (**c**) twisting cycle at a twisting angle of 180^{o}.

Table S1. Specific capacity and energy density of representative lithium-air (oxygen) batteries. The specific capacity was calculated based on the weight of air electrode; the energy density was calculated based on the total weight of air electrode and resultant Li_2O_2.

Configuration	Air electrode	Specific capacity (mAh/g)	Energy density (Wh/kg)	Ref.
Rigid	N-Fe-MOF	5300	/	S1
Rigid	Hierarchically porous carbon	11060	2784	S2
Rigid	Hollow carbon fibers	4720	~2500	S3
Flexible	TiO_2 NAs/CT	~3000	/	S4
Flexible	Paper-ink	~6500	/	S5
Flexible	Aligned CNT sheets	12470	2457	S6
Flexible and stretchable	Aligned CNT sheets	7111	2540	This work

N-Fe-MOF: MOF-template nitrogen-iron catalysts; TiO_2 NAs/CT: TiO_2 nanowire arrays grown onto carbon textiles.

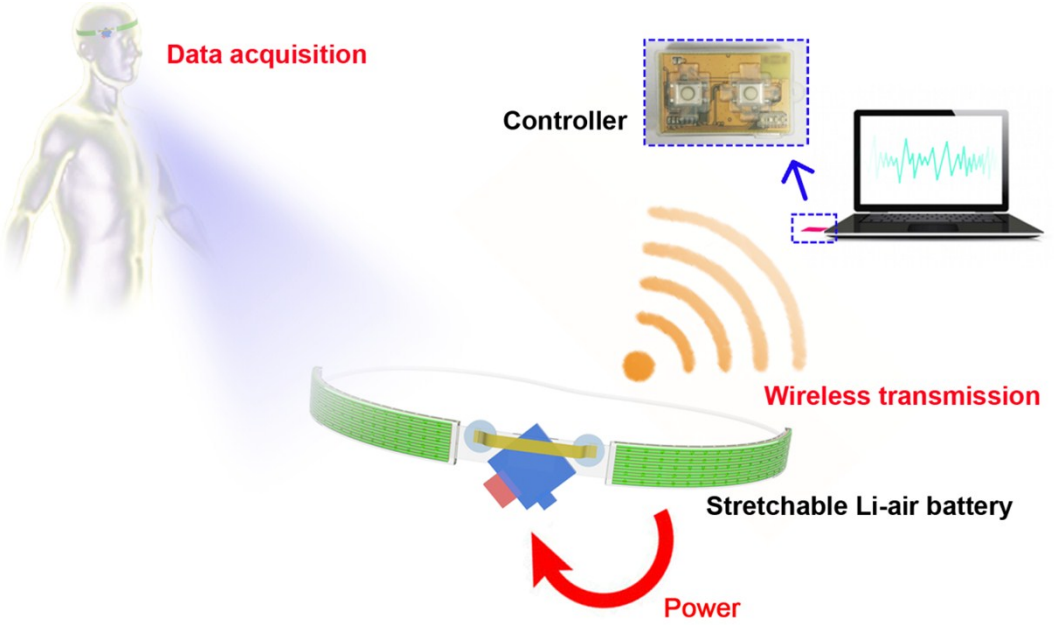

Figure S12. Schematic illustration to the collection of physiological signals by the wearable physiological monitoring system.

Supplementary References

[S1] Q. Li, P. Xu, W. Gao, S. Ma, G. Zhang, R. Cao, J. Cho, H. L. Wang, G. Wu, *Adv. Mater*. 2014, **26**, 1378.

[S2] Z. L. Wang, D. Xu, J. J. Xu, L. L. Zhang, X. B. Zhang, *Adv. Funct. Mater*. 2012, **22**, 3699.

[S3] R. R. Mitchell, B. M. Gallant, C. V. Thompson, Y. Shao-Horn, *Energy Environ. Sci.* 2011, **4**, 2952.

[S4] Q. Liu, J. Xu, D. Xu, X. Zhang, *Nat. Commun*. 2015, **6**, 7892.

[S5] Q. C. Liu, L. Li, J. J. Xu, Z. W. Chang, D. Xu, Y. B. Yin, X. Y. Yang, T. Liu, Y. S. Jiang, J. M. Yan, X. B. Zhang, *Adv. Mater*. 2015, **27**, 8095.

[S6] Y. Zhang, L. Wang, Z. Guo, Y. Xu, Y. Wang, H. Peng, *Angew. Chem. Int. Ed*. 2016, **55**, 4487.